

Placental autophagy regulation by the BOK-MCL1 rheostat

Manpreet Kalkat,^{1,2} Julia Garcia,¹ Jessica Ebrahimi,¹ Megan Melland-Smith,^{1,2} Tullia Todros,³ Martin Post,^{2,4,5} and Isabella Caniggia^{1,2,6,*}

¹Lunenfeld-Tanenbaum Research Institute; Mount Sinai Hospital; Toronto, ON CA; ²Department of Physiology; University of Toronto; Toronto, ON CA;

³Department of Obstetrics and Gynecology; University of Turin; Turin, Italy; ⁴Department of Pediatrics; University of Toronto; Toronto, ON CA; ⁵The Hospital for Sick Children; Toronto, ON CA; ⁶Department of Obstetrics and Gynecology; University of Toronto; Toronto, ON CA

Keywords: placenta, MCL1, BOK, oxidative stress, autophagy, preeclampsia

Abbreviations: ACTB, actin, beta; AMC, age-matched control; BafA₁, bafilomycin A₁; BECN1, Beclin 1, autophagy-related; BH, BCL2 homology; BOK, BCL2-related ovarian killer; CASP3, caspase 3; CT, cytotrophoblast cells; E, endothelium; GFP, green fluorescent protein; IUGR, intrauterine growth restriction; LC3B/LC3B-II, cleaved and lipidated form of microtubule-associated protein 1 light chain 3 beta (MAP1LC3B); MCL1, myeloid cell leukemia sequence 1 (BCL2-related); NO, nitric oxide; PE, preeclampsia; ST, syncytium/syncytiotrophoblast cells; TC, term control; SNP, sodium nitroferricyanide (III)

Autophagy is the catabolic degradation of cellular cytoplasmic constituents via the lysosomal pathway that physiologically elicits a primarily cytoprotective function, but can rapidly be upregulated in response to stressors thereby inducing cell death. We have reported that the balance between the BCL2 family proteins BOK and MCL1 regulates human trophoblast cell fate and its alteration toward cell death typifies preeclampsia. Here we demonstrate that BOK is a potent inducer of autophagy as shown by increased LC3B-II production, autophagosomal formation and lysosomal activation in HEK 293. In contrast, using JEG3 cells we showed that prosurvival MCL1 acts as a repressor of autophagy via an interaction with BECN1, which is abrogated by BOK. We found that MCL1-cleaved products, specifically MCL1c157, trigger autophagy while the splicing variant MCL1S has no effect. Treatment of JEG3 cells with nitric oxide donor SNP resulted in BOK-MCL1 rheostat dysregulation, favoring BOK accumulation, thereby inducing autophagy. Overexpression of MCL1 rescued oxidative stress-induced autophagy. Of clinical relevance, we report aberrant autophagy levels in the preeclamptic placenta due to impaired recruitment of BECN1 to MCL1. Our data provided the first evidence for a key role of the BOK-MCL1 system in regulating autophagy in the human placenta, whereby an adverse environment as seen in preeclampsia tilts the BOK-MCL1 balance toward the build-up of isoforms that triggers placental autophagy.

Introduction

Autophagy is a self-digestion process that involves the sequestration of cytoplasmic constituents by double-membraned vacuoles, termed autophagosomes, which undergo catabolic degradation after lysosomal fusion.¹ Although basal levels of autophagy in cells are physiological, a variety of stressors, including glucose deprivation and oxidative stress, can rapidly trigger the autophagic machinery.^{2,3} Autophagy dysfunction has been associated with a variety of pathologies including cancer, infection, aging, and neurodegenerative diseases.^{4,5} While it is accepted that autophagy functions as a cytoprotective mechanism, it has been shown that dying cells can undergo massive amounts of autophagy in the absence of apoptotic molecular events, implicating a role for this catabolic process in cell death independent of apoptosis.⁶ Moreover, reports have demonstrated that autophagy can be switched to apoptosis via cleavage of the autophagy-related protein ATG5.⁶ Since autophagy ties together

networks of cellular metabolism and death, it has been recognized as an important player orchestrating cell fate decisions.

The B-cell lymphoma 2 (BCL2) family of proteins, widely recognized as master regulators of cell fate decisions in response to a variety of stimuli, includes prosurvival (BCL2L1, BCL2L2, MCL1) and proapoptotic factors (BAK1, BAX, BOK).⁷ These promiscuous group of proteins can oligomerize with one another via their BCL2 homology (BH) domains,⁷ thereby regulating cell fate. The apoptotic function of the BCL2 proteins is known to result from their localization to the mitochondria; however, they can also localize to other intracellular membranes and organelles, activating other cellular processes including autophagy.⁸ The haploinsufficient tumor suppressor BECN1, a BH3-only BCL2 family member, is central in the crosstalk between apoptosis and autophagy.^{1,9} BECN1 is an essential protein for autophagy as it mediates the cellular signaling upstream of autophagic vesicle formation.¹⁰ Intriguingly, BECN1 serves as a link for the

*Correspondence to: Isabella Caniggia; Email: caniggia@lunenfeld.ca
Submitted: 11/21/2012; Revised: 09/04/2013; Accepted: 09/10/2013
<http://dx.doi.org/10.4161/auto.26452>

interplay between the regulation of autophagy and apoptosis via its interaction with BCL2 and BCL2L1, and more recently, MCL1.^{11,12}

BCL2-related ovarian killer (BOK) is a multidomain proapoptotic BCL2 family member with expression restricted to reproductive organs.^{13,14} Similarly to BAX, BOK contains 3 BCL2 homology domains (BH domains) and a transmembrane domain, which facilitate its proapoptotic activity via mitochondrial depolarization.^{13,15} BOK preferentially binds to Myeloid Cell Leukemia factor 1 (MCL1), a prosurvival BCL2 family protein that is also highly expressed in reproductive tissues.¹⁶ However, the *MCL1* gene is prone to alternative splicing, which results in the formation of proapoptotic MCL1S.¹⁷ In addition, the full-length MCL1 protein contains 2 PEST (proline, glutamic acid, serine, and threonine) regions that are subjected to caspase cleavage, thereby generating proapoptotic cleaved products and inducing rapid MCL1 turnover.^{16,18}

Preeclampsia (PE) is a serious placental disorder complicating 3% to 7% of all pregnancies, that remains one of the leading causes of maternal and fetal morbidity and mortality.¹⁹ Preeclamptic pathology is characterized by shallow trophoblast invasion into the maternal decidua resulting in deficient spiral artery remodelling, which in turn leads to aberrant placental blood flow and oxidative stress within the placental tissue.²⁰ In vivo and in vitro studies have shown that placental hypoxia/oxidative stress contributes to the preeclamptic phenotype of trophoblast cells, which is characterized by increased trophoblast proliferation and death.²¹⁻²³ While efforts have been made to understand the involvement of BCL2 family members in driving mitochondrial-dependent cell death in the developing human placenta and its associated disorders,^{23,24} the contribution of these cell fate regulatory proteins to placental autophagy in normal and pathological conditions remains to be elucidated. We have previously addressed the role of the BOK-MCL1 system in regulating trophoblast cell fate in placental development and disease.¹⁶ In particular, we have shown that in preeclamptic placenta the BOK-MCL1 rheostat is tilted toward the accumulation of prodeath isoforms, resulting in increased apoptosis and a hyperproliferative status of trophoblast cells.^{16,23,24} In this study, we sought to unravel the complex roles of the BOK-MCL1 system in regulating placental autophagy.

Results

BOK is a novel inducer of autophagy

Emerging evidence highlights a role for BCL2 family members in regulating autophagy in the context of both cell survival and death.^{25,26} Previously, we reported that proapoptotic BOK contributes to both excessive trophoblast cell death and proliferation typical of placentas from PE pregnancies^{23,24} and hence we examined its role in autophagic regulation. Since BOK is a protein that rapidly induces apoptosis at high concentrations¹³ we used a tetracycline-inducible HEK 293 Flp-In T-Rex cell system that allowed for controlled expression of BOK.²³ In our first set of experiments, we established that induction of GFP-tagged BOK expression by a 24 h doxycycline treatment resulted in increased expression of the autophagic marker LC3B-II (GFP-BOK:

4.59 fold \pm 1.03 increase compared with control GFP cells; $P < 0.001$) (Fig. 1A). Induction of GFP alone by doxycycline had no effect on LC3B-II formation (Fig. 1A). Electron microscopy of GFP and GFP-BOK expressing cells established the presence of autophagosomes in BOK expressing cells while cytoplasmic vacuolization was absent in GFP control cells (Fig. 1B). Cells were subsequently stained with LysoTracker® Red, a live-cell dye used for labeling acidic organelles indicative of increased lysosomal activity. Following doxycycline treatment, cells expressing GFP-BOK displayed increased lysosomal/autophagosomal activity when compared with GFP-expressing control cells (Fig. 2A, left panels). The mitochondrial presence of BOK was verified by immunofluorescence analysis showing association of GFP-BOK with cytochrome C, a resident of the inner mitochondrial membrane (Fig. 2A, right panel). To confirm the presence of autophagic flux,²⁷ cells were treated with bafilomycin A₁ (BafA₁), an inhibitor of autophagic vesicle fusion with the lysosomal machinery.²⁷ Hindrance of lysosomal degradation by BafA₁ resulted in the accumulation of LC3B-II in BOK-expressing cells following treatment with doxycycline, as compared with vehicle-treated cells and untransfected cells treated with doxycycline alone (Fig. 2B). BafA₁ treatment also induced LC3B-II build-up relative to vehicle alone although to a lesser extent than that observed with doxycycline induction (Fig. 2B). SQSTM1/p62, a protein that links LC3 to ubiquitinated substrates, serves as a marker of autophagic flux as it first accumulates in the autophagosome and then upon autophagosome-lysosome fusion is promptly degraded, indicating completion of autophagy.²⁷ Hence, we examined SQSTM1 expression in the BOK-expressing cells in the presence or absence of doxycycline following treatment with BafA₁. As anticipated doxycycline induction of BOK decreased SQSTM1 expression, while BafA₁ inhibition of autophagosomal flux blocked SQSTM1 degradation in cells in the presence or absence of doxycycline (Fig. 2B). Confocal analysis revealed that treatment of cells with BafA₁ resulted in increased positive cytoplasmic SQSTM1 signal that exhibited a punctated staining compared with control cells (Fig. 2C). Also, induction of GFP-BOK expression by doxycycline in BafA₁-treated cells showed colocalization of SQSTM1 with BOK (Fig. 2C). We next evaluated the consequences of BOK depletion on the expression of autophagic markers in choriocarcinoma JEG3 cells, a human cell line of placental origin, using a siRNA knockdown approach. This approach has been previously used in our laboratory with a protein knockdown efficiency in cells of 50% to 60%.^{23,28} The knockdown of BOK, using 2 different duplexes (D1–2), resulted in a reduction of both LC3B-II and SQSTM1 protein expression relative to control scrambled (SS) siRNA-treated cells (Fig. 2D) further corroborating the physiological involvement of BOK in the regulation of autophagy. Taken together, these data indicated that BOK functions as an inducer of autophagy.

BOK disrupts the interaction between MCL1 and BECN1

We have previously reported that a balance between proapoptotic BOK and prosurvival MCL1 is critical for trophoblast cell homeostasis and that MCL1 is capable of rescuing BOK-induced trophoblast cell death.¹⁶ Notably, MCL1 has been found to play an important role in suppressing autophagy in cortical

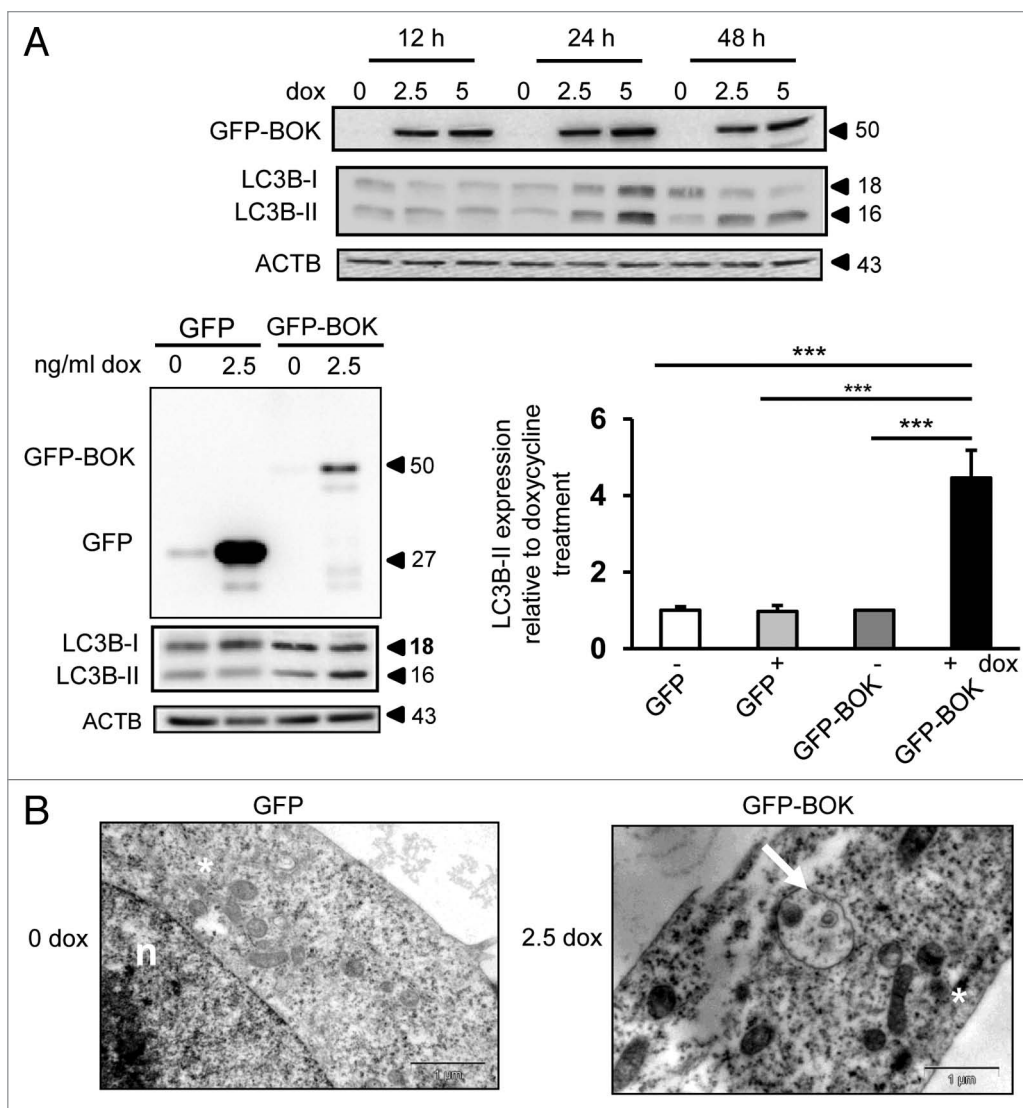


Figure 1. BOK is a novel inducer of autophagy. **(A)** Upper panel: Representative immunoblot for GFP-BOK and LC3B-II expression in HEK293Trex cells stably transfected with GFP-BOK and treated with doxycycline (2.5 and 5 ng) for different times (12, 24, and 48 h) to induce GFP-BOK expression. Lower left panel: Representative immunoblot for GFP or GFP-BOK in HEK 293Trex cells stably transfected with either GFP or GFP-BOK following 2.5 ng/mL doxycycline treatment for 24 h. Lower right panel: Densitometric analysis of LC3B-II expression normalized to ACTB in HEK293Trex cells expressing GFP-BOK after 2.5 ng/mL doxycycline treatment. Data are expressed as fold-change relative to control vehicle treated GFP-BOK cells*** $P < 0.001$, $n = 3$ experiments run in triplicate). **(B)** Electron micrographs of HEK293Trex cells expressing either GFP or GFP-BOK after 2.5 ng/ml doxycycline treatment. Autophagosomal formation in cells expressing GFP-BOK is indicated by white arrows.*: mitochondria; n: nucleus. $n = 3$ experiments performed in duplicate.

neurons.¹² Therefore, we examined the contribution of MCL1 in regulating BOK-induced cell autophagy. First, we examined the interaction of BOK-MCL1 using the inducible 293Trex cells stably transfected with either GFP-BOK or GFP. Confocal analysis showed extensive colocalization of BOK and MCL1 in the cytoplasm of the doxycycline-induced GFP-BOK, but not GFP, 293Trex cells (Fig. 3A). Induction of GFP-BOK by doxycycline resulted in a small but not significant decrease in MCL1 levels when compared with vehicle and GFP alone (Fig. 3B). Since previous studies have demonstrated that prosurvival MCL1 directly interacts with BECN1,^{11,12} we next determined whether BOK exerts its autophagic effect by displacing BECN1 from

MCL1. Immunoprecipitation experiments demonstrated that MCL1 associated with BECN1 in control 293Trex-GFP cells with and without doxycycline induction; however, following induction of BOK by doxycycline, the interaction between MCL1 and BECN1 was disrupted (Fig. 3C). In order to substantiate the changes in the association of these proteins, supernatants remaining after immunoprecipitation of the lysates with BECN1 were immunoblotted for MCL1. Densitometric analysis of the blots revealed a significant increase in MCL1 protein content in the supernatant fraction of cells expressing GFP-BOK compared with those expressing GFP (Fig. 3D), corroborating the interference of BOK with the MCL1-BECN1 interaction.

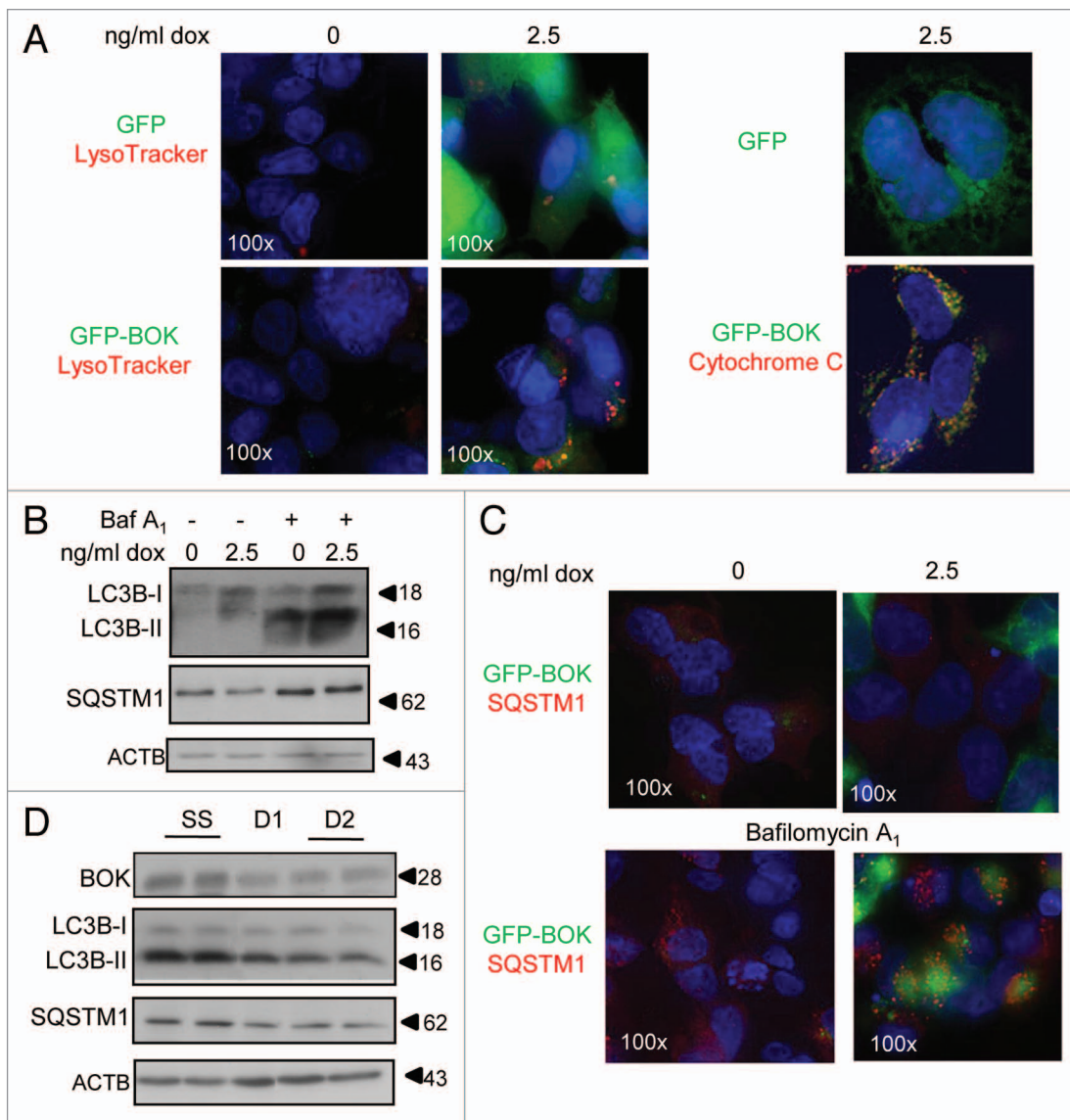


Figure 2. BOK induces lysosomal activity and autophagic flux. **(A)** Left panels: Immunofluorescence analysis of lysosomal marker LysoTracker® Red (red) in HEK293T cells expressing either GFP or GFP-BOK following treatment with vehicle or 2.5 ng/mL doxycycline. Nuclei are counterstained with DAPI (blue); $n = 4$ different experiments performed in duplicate. Right panels: Immunofluorescence analysis of GFP, GFP-BOK and cytochrome C in HEK293T cells expressing either GFP or GFP-BOK following treatment with 2.5 ng/mL doxycycline; representative images of 3 separate experiments. **(B)** HEK293T cells stably transfected with GFP-BOK were treated with doxycycline with and without BafA₁ for 24 h and autophagic flux was monitored by immunoblotting for LC3B-II and SQSTM1; representative immunoblots of 3 separate experiments. ACTB immunoblot demonstrates equal protein loading. **(C)** Immunofluorescence staining for SQSTM1 (red signal) in HEK293T cells expressing either GFP or GFP-BOK (green signal) after treatment with 2.5 ng/mL doxycycline in the presence or absence of BafA₁. Nuclei are visualized with DAPI (blue signal). **(D)** LC3B-II and SQSTM1 protein expression in JEG3 cells following BOK siRNA treatment; representative immunoblots of 3 separate experiments. ACTB immunoblot demonstrates equal protein loading.

The dynamic role of MCL1 isoforms as regulators of autophagy

Since prosurvival MCL1 appears to act as an inhibitor of autophagy in neuronal cells,¹² we determined its autophagy function in trophoblast cells by a series of gain-and loss-of-function experiments using choriocarcinoma JEG3 cells. Transient overexpression of MCL1 in JEG3 cells was accompanied by a significant reduction in LC3B-II formation relative to control cells transfected with empty vector (Fig. 4A). Knockdown of

MCL1, using 2 different siRNA sequences targeted against MCL1 mRNA, resulted in a marked reduction of MCL1 protein [73% for duplex 1 (D1) and 61% for duplex 2 (D2)] relative to cells treated with control scrambled sequences (Fig. 4B). The MCL1 knockdown was accompanied by a significant increase in LC3B-II protein (D1: 1.79 ± 0.32 -fold increase vs. SS, D2: 1.64 ± 0.19 -fold increase vs. SS, $P < 0.05$). Increased lysosomal/autophagosomal activity, visualized with LysoTracker® Red following siRNA silencing of MCL1, substantiated increased

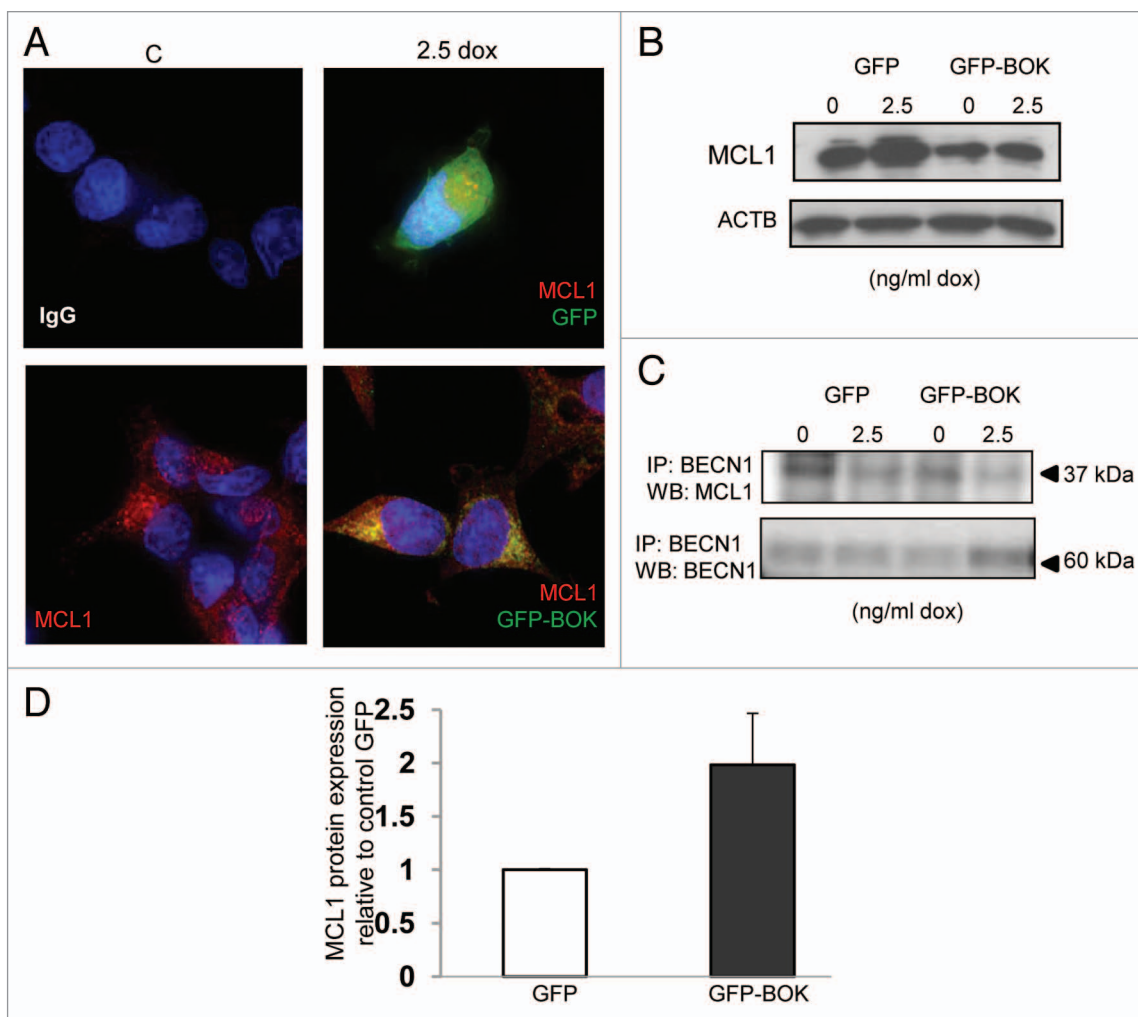


Figure 3. BOK disrupts the interaction between MCL1 and BECN1. **(A)** Immunofluorescence staining for MCL1 (red signal) in HEK293T cells expressing either GFP or GFP-BOK (green signal) after treatment with 2.5 ng/mL doxycycline. Nuclei are visualized with DAPI (blue signal). **(B)** Representative immunoblot for MCL1 in lysates from HEK 293T cells stably transfected with either GFP or GFP-MtdL following 2.5 ng/mL doxycycline treatment. **(C)** Representative immunoprecipitation of BECN1 followed by immunoblotting for either MCL1 or BECN1 in HEK293T cells treated with 2.5 ng/ml doxycycline to induce GFP or GFP-BOK. **(D)** Densitometric analysis of MCL1 protein content in supernatants of lysates from HEK293T cells treated with 2.5 ng/ml doxycycline to induce GFP or GFP-BOK after immunoprecipitation for BECN1 (n = 3 experiments in duplicate).

autophagy (Fig. 4C). Hence, in this model of human placental cells, MCL1 functions as a repressor of autophagy.

In PE placentas the balance between prodeath BOK and prosurvival MCL1 is tilted toward the accumulation of proapoptotic MCL1 splicing variant (MCL1S) and proapoptotic cleaved MCL1 products together with increased levels of BOK.¹⁶ As MCL1S and cleaved MCL1 proteins retain the BH3 domains essential for BCL2 family protein interactions, we next determined their role in regulating autophagy. Specific constructs for MCL1 products cleaved at residues 157 and 127, respectively, as well as MCL1S were generated for transient expression. JEG3 cells were transfected with either control pcDNA3.1 vector or constructs for MCL1c157 and MCL1c127 as well as MCL1S. Increased expression of both MCL1S and cleaved products was confirmed by immunoblotting (Fig. 5A). LC3B-II and cleaved CASP3 levels were monitored to assess autophagic and apoptotic activation (Fig. 5B). Surprisingly, MCL1c157 and to

a lesser extent MCL1c127, but not MCL1S, induced autophagy as demonstrated by a 2.5-fold increase in LC3B-II formation relative to cells transfected with empty vector (Fig. 5B). In contrast, only the MCL1S isoform increased cleaved CASP3 levels (Fig. 5B). The effect of MCL1c157 on autophagy was most profound after 24 h of transfection (Fig. 5B, left bottom panel). The effect of MCL1c157 upon autophagy was further validated with LysoTracker[®] Red, which demonstrated an increase in the number of acidic lysosomes post-transfection with MCL1c157 construct when compared with cells transfected with control empty vector (Fig. 5C). Inhibition of autophagic flux with BafA₁ resulted in increased LC3B-II and SQSTM1 accumulation in JEG3 cells transiently transfected with MCL1c157 and MCL1c127 relative to control empty vector (Fig. 5D).

Autophagy is elevated in preeclampsia

Placentas from PE pregnancies have aberrant levels of BOK and cleaved MCL1.^{16,24} Therefore, we examined the levels of

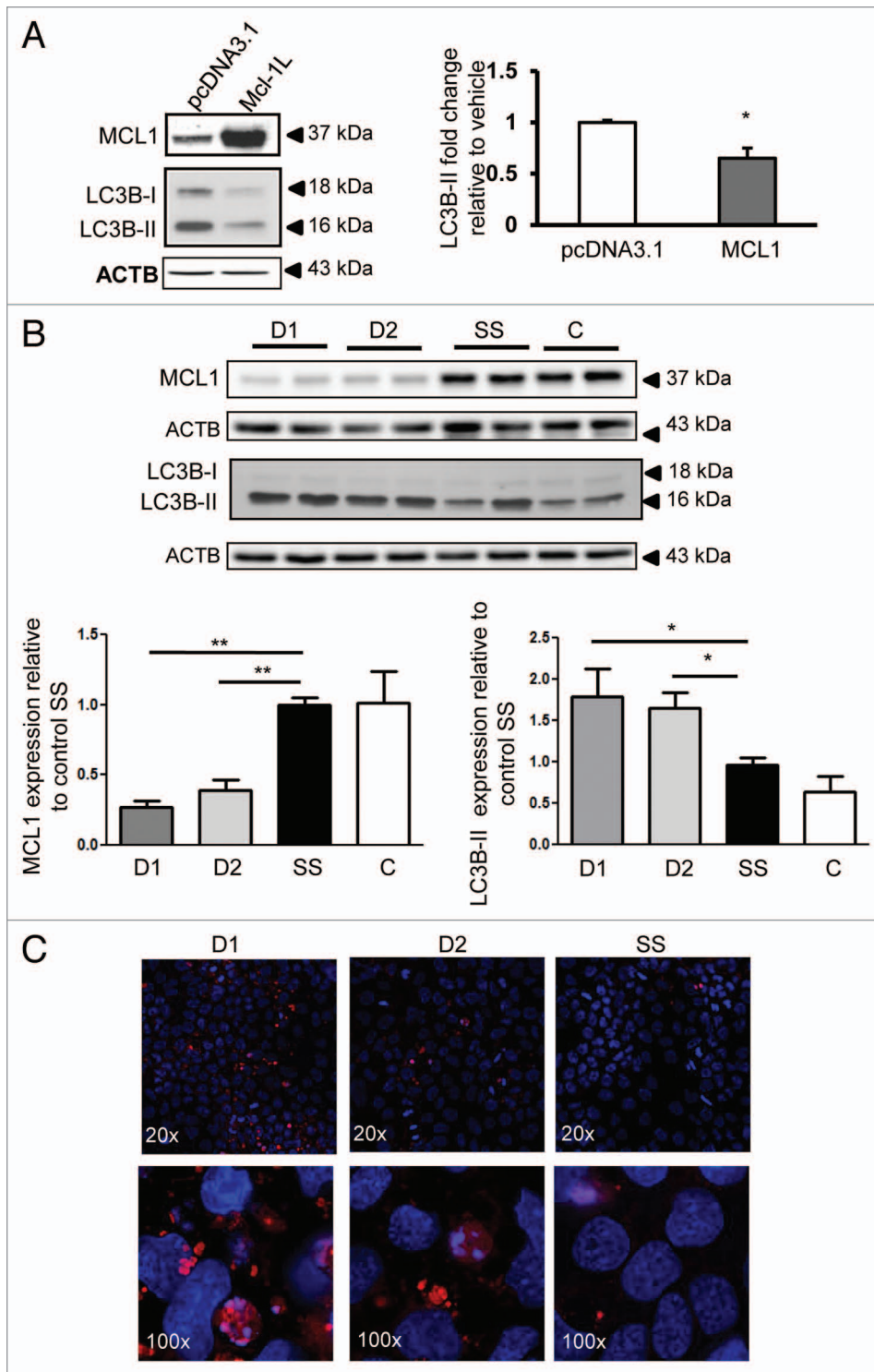


Figure 4. MCL1 is an inhibitor of autophagy. **(A)** Left panel: Representative immunoblot for MCL1 and LC3B-II in JEG3 choriocarcinoma cells transiently transfected with either empty pcDNA3.1 or pcDNA3.1MCL1 vectors. Right panel: Densitometric analysis of LC3B-II normalized to ACTB in JEG3 cells transiently transfected with control empty vector and MCL1 construct. * $P < 0.05$, $n = 3$ experiments in triplicate. **(B)** Upper panel: Representative immunoblots for MCL1 and LC3B-II in JEG3 cells treated with MCL1 siRNA. D1: MCL1 siRNA duplex 1; D2: MCL1 siRNA duplex 2; SS: scrambled sequence control; C: untreated control. Lower left panel: Densitometric analysis of MCL1 normalized to ACTB and expressed as fold change relative to SS. Right panel: Densitometric analysis of LC3B-II normalized to ACTB and expressed as fold change relative to SS. * $P < 0.05$, ** $P < 0.01$, $n = 4$ experiments in triplicate. **(C)** LysoTracker[®] Red staining in JEG3 cells treated with MCL1 siRNA. D1: MCL1 siRNA duplex 1; D2: MCL1 siRNA duplex 2; SS: scrambled sequence control; C: untreated control cells. Nuclei were stained with DAPI (blue signal).

autophagy in placenta from PE, age-matched (AMC), and term control (TC) pregnancies. Immunoblotting for LC3B-II revealed a significant increase in severe early onset PE placentas when compared with both AMC and TC placentas (Fig. 6A: 2.05 ± 0.47 fold increase relative to AMC ($P < 0.01$) and 7.54 ± 0.82 fold increase relative to TC ($P < 0.001$). No significant changes in LC3B-II expression were observed between AMC and TC.

To determine if the increased autophagy observed in PE placentas is dependent upon changes in MCL1-BECN1 interactions, we determined BECN1 protein expression and its association with MCL1. Western blot analysis revealed that both BECN1 and BOK levels were markedly increased in PE placentas relative to AMC (Fig. 6B, upper panels). Immunoprecipitation experiments showed that, while expression of BECN1 in control placentas is minimal, the majority of this protein complexed with MCL1 in AMC samples. The opposite was found in PE placentas where, despite high levels of BECN1, no interaction with MCL1 was detected, indicating a potential contribution of this rheostat to the autophagy phenotype (Fig. 6B, bottom panel). This finding was corroborated by immunofluorescence staining revealing that BECN1 is expressed in the trophoblastic compartment of the placenta and colocalizes with MCL1 in AMC, but not in PE, placentas (data not shown).

Electron microscopy further confirmed the elevated autophagy levels in PE placentas. While AMC placentas retained an organized syncytial appearance with a well-maintained microvillous membrane (mvm) the syncytial layer of PE placentas was highly vacuolated and the mvm highly disorganized (Fig. 6C). Ultrastructurally, autophagosomes were identified by their characteristic double-membraned appearance and cytoplasmic contents contained within a vacuole. A notable

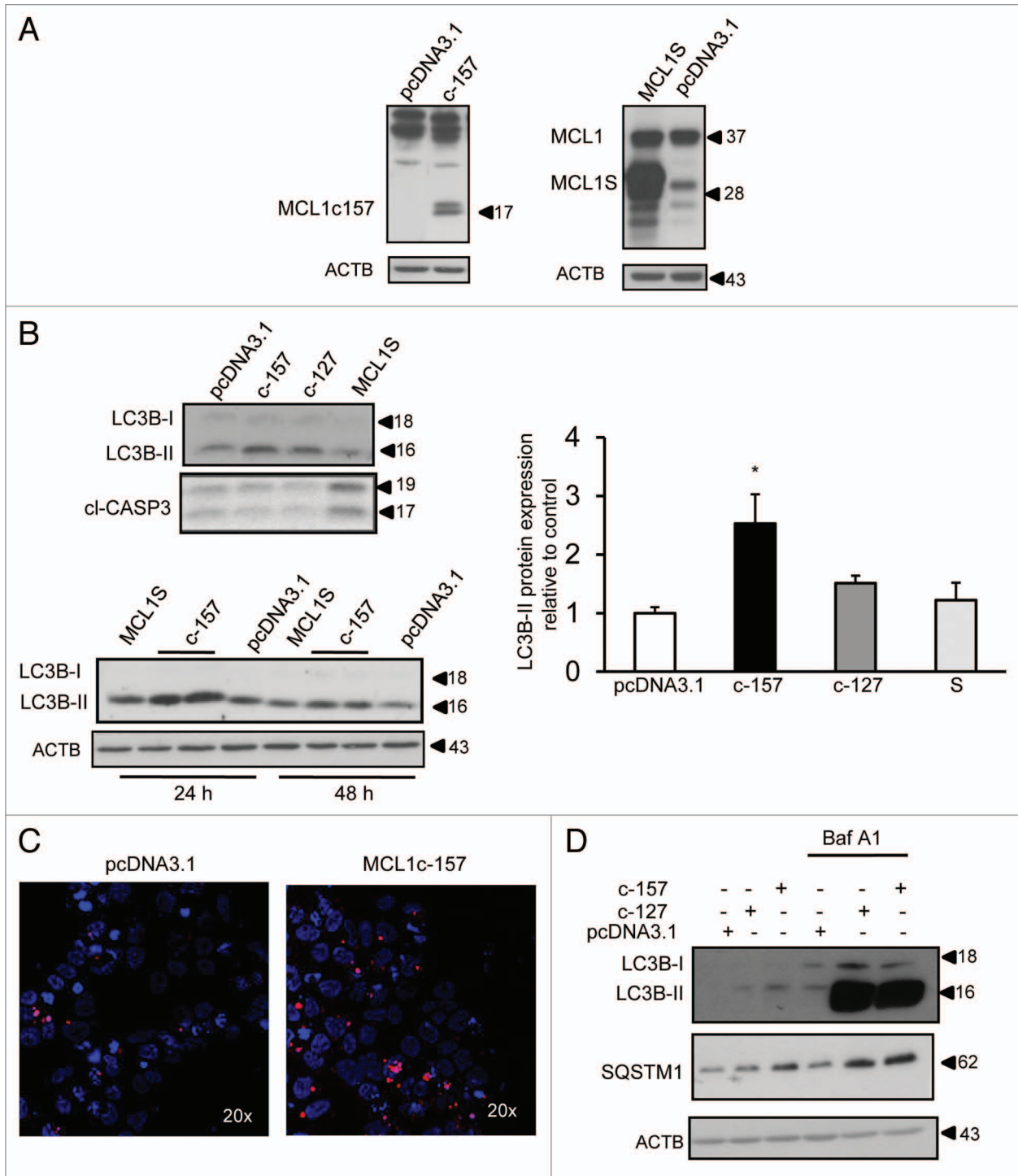


Figure 5. MCL1 cleavage product MCL1c157 promotes lysosomal activity and induces autophagy. **(A)** Representative immunoblots for MCL1c157 and MCL1S using an MCL1 antibody following transient transfection of JEG3 cells with either pcDNA3.1MCL1c157, pcDNA3.1MCL1S or empty pcDNA3.1 constructs. **(B)** Left panel: Representative immunoblots for LC3B-II and cleaved CASP3 (cl-CASP3) in JEG3 cells transiently transfected with MCL1c157, MCL1c127, MCL1S and control pcDNA3.1 constructs. Right panel: Densitometric analysis of LC3B-II protein expression normalized to ACTB in JEG3 cells transiently transfected with MCL1c157, MCL1c127, and MCL1S. (n = 3 separate experiments performed in triplicate; **P < 0.008). **(C)** LysoTracker[®] Red staining in JEG3 cells transfected with either control pcDNA3.1 or MCL1c157. Nuclei are visualized with DAPI (blue signal). **(D)** Representative immunoblots for LC3B-II and SQSTM1 in JEG3 cells transiently transfected with either control pcDNA3.1 or MCL1c157 or MCL1c127 constructs in the presence or absence of the autophagic flux inhibitor BafA₁. ACTB immunoblot demonstrates equal protein loading.

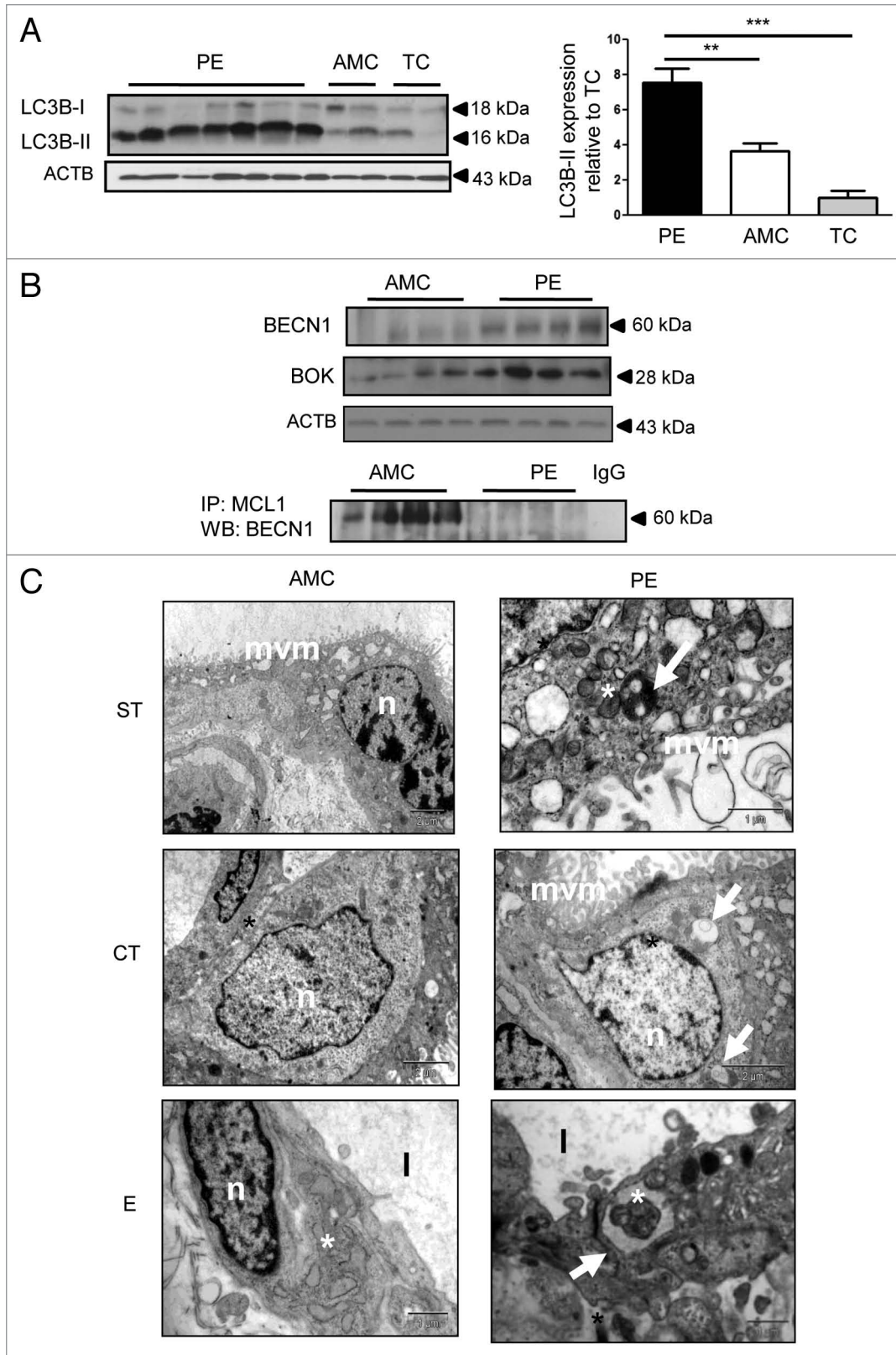


Figure 6. Autophagy is elevated in preeclamptic placentas. **(A)** Left panel: Representative immunoblot for LC3B-II in PE, AMC and TC placentas. ACTB immunoblot demonstrates equal protein loading. Right panel: Densitometric analysis of LC3B-II protein content normalized to ACTB and expressed as fold change relative to TC $**P < 0.01$, $***P < 0.001$, (PE, $n = 14$; AMC, $n = 8$; TC, $n = 4$), AMC, age-matched control; PE, preeclampsia, TC, term control. **(B)** Representative immunoblot for BECN1, BOK, and MCL1-BECN1 association as assessed by immunoprecipitation of MCL1 and followed by western blotting with BECN1 in PE vs. AMC placenta, (PE, $n = 12$; AMC, $n = 10$). **(C)** Representative electron micrographs from normal (AMC, $n = 3$) and pathological (PE, $n = 4$) placental sections. Autophagosomes are indicated with white arrows. ST, syncytiotrophoblast; CT, cytotrophoblast; E, endothelium; mvm, microvillous membrane; n, nucleus; *, mitochondria.

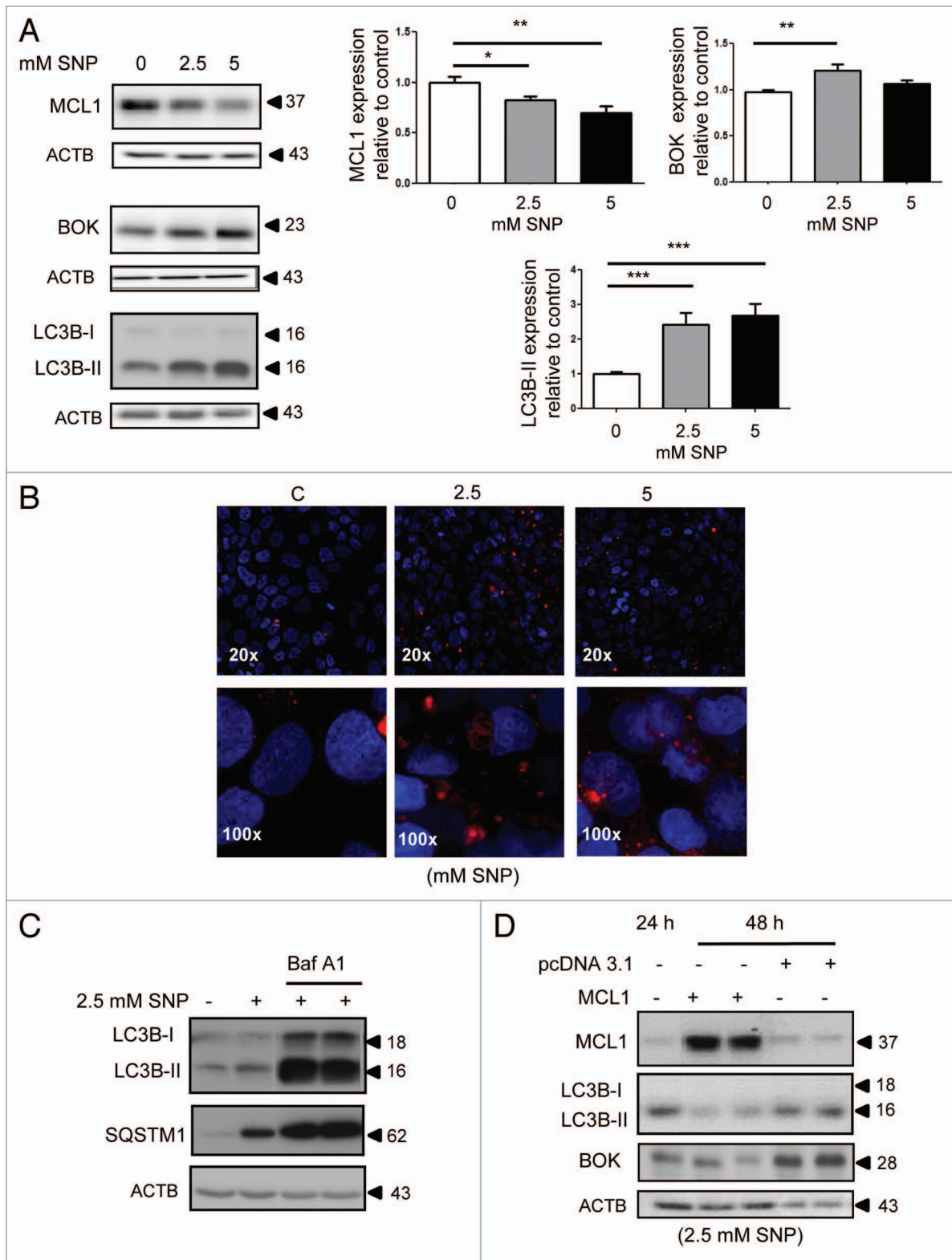


Figure 7. Oxidative stress induces autophagy via alterations in BOK-MCL1 rheostat. **(A)** Left panel: Representative immunoblots for MCL1, BOK and LC3B-II in JEG3 choriocarcinoma cells after 2.5 and 5 mM SNP treatment. ACTB immunoblots demonstrate equal protein loading. Right panel: Densitometric analysis of MCL1, BOK and LC3B-II protein expression normalized to ACTB and expressed as fold-change relative to untreated control. * $P < 0.05$, ** $P < 0.01$, *** $P < 0.001$. MCL1, $n = 6$ experiments in triplicate; BOK, $n = 4$ experiments in triplicate; LC3B-II, $n = 6$ experiments in triplicate. **(B)** LysoTracker[®] Red staining of JEG3 cells after 2.5 and 5 mM SNP treatment. Nuclei were visualized with DAPI (blue signal), $n = 3$ experiments in duplicate. **(C)** Representative immunoblots for LC3B-II and SQSTM1 in JEG3 cells after 2.5 and 5 mM SNP treatment in the presence or absence of the autophagic flux inhibitor BafA₁. ACTB immunoblot demonstrates equal protein loading. **(D)** Representative immunoblot for MCL1, BOK and LC3B-II in JEG3 cells transfected with either MCL1 or empty pcDNA3.1 vector (EV) after 2.5 mM SNP treatment. Experiment was repeated twice with similar results.

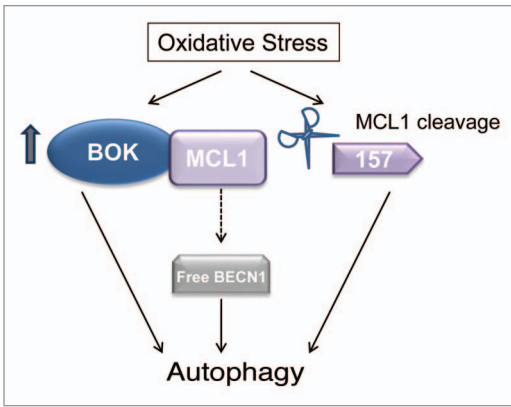


Figure 8. Putative model for altered BOK-MCL1 rheostat in autophagic regulation in preeclamptic placentas. Increased BOK expression following oxidative stress insult, leads to induction of autophagy directly or indirectly by a mechanism that involves BOK sequestration of MCL1, thereby freeing BECN1. Furthermore, oxidative stress-induced MCL1 cleavage further triggers autophagy.

increase in autophagosomal structures was detected in both syncytial layers (ST, CT) and endothelium (E) in PE placentas when compared with AMC placentas (Fig. 6C). Intriguingly, evidence for mitophagy, that characterizes the recycling of mitochondria, was also observed in sections from PE placentas.

Oxidative damage induces autophagy via alterations in BOK-MCL1 balance

To determine if increased autophagy in PE may be the result of increased oxidative stress typical of this pathology,^{20,21} JEG3 cells were treated with sodium nitroprusside (SNP), a compound that triggers a status of intracellular oxidative stress.²⁹ Treatment of JEG3 cells with 2.5 and 5 mM of SNP resulted in a dose-dependent decrease of MCL1 expression (Fig. 7A). Conversely, following SNP treatment, BOK protein levels significantly increased relative to control. These changes in MCL1 and BOK protein expression in response to SNP treatment correlated with a significant increase in LC3B-II levels (2.5 mM SNP: 2.43 ± 0.33 fold increase relative to control $P < 0.001$; 5 mM SNP: 2.68 ± 0.35 fold increase relative to control, $P < 0.001$). Autophagic induction in response to SNP treatment was further confirmed with LysoTracker® Red staining, i.e., increased lysosomal formation/activity in cells treated with SNP as compared with control untreated cells (Fig. 7B). Inhibition of autophagic flux with BafA₁ resulted in increased LC3B-II and SQSTM1 accumulation in JEG3 cells following treatment with SNP (Fig. 7C). We then investigated if the autophagic effect of SNP could be rescued by overexpression of MCL1 protein. Overexpression of MCL1 decreased BOK levels and prevented SNP-induced LC3B-II formation, demonstrating that SNP triggered autophagy in JEG3 cells is largely dependent upon the BOK-MCL1 balance (Fig. 7D).

Discussion

In the present study, we demonstrated for the first time that proapoptotic BOK, a BCL2 family member, is a powerful inducer

of autophagy. While its prosurvival partner MCL1 functions as a repressor of this lysosomal degradation pathway, cleaved products of MCL1, specifically MCL1c157, trigger autophagy. In addition, we show that MCL1 is capable of rescuing oxidative stress-induced autophagy. Of clinical relevance, we report aberrant autophagy levels in severe preeclamptic placentas due to impaired recruitment of BECN1 to MCL1, most likely caused by BOK interference. Hence, in PE, the oxidative stress milieu, known to tilt the BOK-MCL1 system toward the accumulation of cell death-inducing isoforms, triggers placental cell autophagy, thereby contributing to the pathogenesis of this disease.

In the human placenta, the BOK-MCL1 system is central to survival and proliferation of trophoblast cells, necessitating the question of whether their interplay also plays a role in regulating autophagy in this tissue.^{16,23,24} Our finding of BOK being able to induce LC3B-II expression, autophagosomal formation and lysosomal activation in HEK293 cells implicates a novel role for this proapoptotic protein in the regulation of autophagy. Furthermore, our results of altered SQSTM1 degradation following overexpression or knockdown of BOK as well as increased LC3B-II and SQSTM1 accumulation following inhibition of autolysosome formation with BafA₁, are consistent with a role for BOK in regulating autophagic flux through the entire process of autophagy. Recent reports have demonstrated that a complex crosstalk exists between regulators of apoptosis and autophagy that is mediated by the haploinsufficient tumor suppressor BECN1, a BH3-only protein^{1,9} with no apparent apoptotic effects.^{10,11,30} BECN1 has been reported to interact with several prosurvival members of the BCL2 family proteins, including BCL2, BCL2L1, BCL2L2, and to a lesser extent with MCL1.^{11,12} The interaction of BECN1 with BCL2 has been shown to inhibit autophagy via sequestration of BECN1 from its autophagy activating complex with the lipid kinase class III PtdIns3K, which contains PIK3C3/Vps34 as the catalytic subunit.³⁰ Conversely, proapoptotic BH3-only proteins, including BNIP3, PMAIP1, BBC3, BCL2L11, and BAD, have been shown to indirectly induce autophagy by binding and sequestering the prosurvival protein BCL2, thereby preventing its interaction with BECN1.³¹ Our immunoprecipitation data suggests that recruitment of MCL1 by BOK interferes with MCL1-BECN1 interactions, thereby freeing BECN1 that subsequently induces autophagy. Alternatively, similarly to BCL2 and BCL2L1, which induce cytoprotective- and cell death-promoting autophagy via a mechanism independent of BECN1,³² BOK alone may directly trigger autophagy (Fig. 8). Independent of the mechanism, however, the multidomain BH3 family member BOK can be added to the growing list of proapoptotic BCL2 family proteins implicated in autophagic induction.

MCL1 has recently been reported to inhibit autophagy in postmitotic cortical neurons.¹² In line with this report, our data indicate that in JEG3 choriocarcinoma cells, MCL1 suppresses autophagy (most likely by interacting with BECN1), which is abrogated by either BOK sequestration or MCL1 cleavage (Fig. 8). Intriguingly, caspase-cleavage products of MCL1, specifically MCL1c157, were found to promote autophagy via a

yet undefined mechanism. The MCL1S splicing variant did not affect autophagic activation but induced apoptosis as suggested previously.¹⁶ Many intricacies exist in networks controlling autophagy and apoptosis. For example, calpain-mediated cleavage of ATG5 has been reported to tilt the balance from autophagy to apoptosis³³ and reports have shown that BAX-induced caspase cleavage of BECN1 ablates its autophagic activity.³⁴ Our finding of MCL1c157 being involved in the induction of autophagy further ties together these networks. While full-length MCL1 inhibits apoptosis, caspase-mediated cleavage not only decreases pro-survival MCL1 levels but also results in the accumulation of autophagic MCL1 isoforms. Taken together, our data support a critical role for the BOK-MCL1 system in autophagy and suggests that aberrant MCL1 protein regulation, at the level of both expression and cleavage, can result in autophagic activation in JEG3 choriocarcinoma cells.

Studies on cell death in preeclamptic placentas have thus far reported on trophoblast apoptosis and necrosis, but have not systematically examined the relative contribution of autophagy and its potential regulatory mechanisms in trophoblast cell homeostasis. In this study, we provide evidence that autophagy levels are markedly elevated in placentas from severe preeclamptic pregnancy, corroborating findings from a previous report.³⁵ A recent report indicates that intrauterine growth restriction (IUGR) placentas exhibit increased autophagy levels;³⁶ however, in the current study, only 20% of placental tissues examined were from preeclamptic pregnancies complicated by IUGR and no differences in markers of autophagy in preeclamptic placentas with and without IUGR were detected. Moreover, we found that the mode of delivery did not affect the placental autophagy outcome in our pathological and age-matched control groups and no differences were found between preterm and term controls. This argues with a previous report showing increased autophagy in placentas obtained from caesarean sections; however, placentas examined in this study were from term-uncomplicated pregnancies.³⁷

Our electron microscopy data provide evidence for autophagy structures in trophoblast cell layers and in the endothelium of chorionic villi vessels. The syncytiotrophoblast layer is the first layer exposed to oxidative damage as it is directly bathed in maternal blood. In PE, the placenta experiences aberrant blood flow, and consequently is exposed to hypoxic injury.^{20,38} The highly vacuolated appearance of the syncytiotrophoblast layer of PE placentas indicates that autophagy is exacerbated in the syncytium, likely in response to oxidative stress thereby contributing to the observed excessive cell death characteristic of this disorder. Autophagy has been implicated in a number of pathologies that exhibit aberrant cell death, and either exacerbating or enhancing this cellular activity has been proposed as a therapeutic for these diseases.^{26,39,40} This highlights a discrepancy in the study of autophagy as unlike apoptosis, the biological outcome of autophagy, as to whether it functions as a pro-death or pro-survival mechanism is unclear and it has been proposed to be dependent upon cellular context. The tissue specificity and functionality of various BCL2 family proteins is further highlighted by the divergent role of MCL1 in autophagy

regulation. While studies conducted in neuronal cells indicate that this pro-survival protein is an inhibitor of autophagy, a report using HCT116 colorectal cancer cells shows that MCL1 is insufficient to inhibit autophagic induction.^{12,32} In the present study, we demonstrated that in PE, despite increased BECN1 levels, BECN1's association to MCL1 is disrupted, likely due to interference by elevated BOK, highlighting a direct involvement of the BOK-MCL1 system in the autophagic activation in this disorder.

Oxidative stress is a major culprit responsible for excessive cell death in PE^{41,42} and we have reported that the tilted balance of the BOK-MCL1 rheostat toward cell death in this disorder is largely dependent upon oxidative stress damage.¹⁶ In the present study, we report that treatment of JEG3 cells with SNP, a nitric oxide (NO) donor which is known to mimic oxidative stress and to activate BCL2 family proteins,^{16,29} reduces and increases the relative abundance of MCL1 and BOK, respectively, which results in increased autophagy. Correcting the BOK-MCL1 balance by overexpression of MCL1 in SNP-treated JEG3 cells, however, abrogates the SNP-induced autophagy. Nitric oxide effects on autophagy are controversial and have shown a cell-dependent role for NO in the regulation of this lysosomal degradation process.^{43,44} While studies using glioma cells have reported that NO inhibits the completion of autophagy,⁴⁵ other reports have demonstrated that in neurons NO increases mitophagy.⁴⁶ Interestingly, we observed that in addition to autophagy, preeclamptic placentas exhibit mitophagy. Previous studies have reported on the role of BNIP3, a BH3-only protein, as regulators of both autophagy and apoptosis in response to hypoxic signaling in cardiac disorders and in cancer.^{47,48} However, our findings suggest that the oxidative stress-altered BOK-MCL1 rheostat is the key inducer of autophagy in PE as we were unable to detect altered levels of BNIP3 in PE placentas (data not shown), suggesting that this BH3-only protein may have distinct tissue-specific functions.

High levels of autophagy in chorionic villi may be an important mechanism by which PE placentas retain functionality in this adverse environment but it is also plausible that this degradation process is predisposing or priming the tissue for an impending death event. While our findings enhance the understanding of autophagic regulation in reproductive tissues, the precise biological relevance of this catabolic process during physiological and pathological conditions in the human placenta remains to be conclusively established. Autophagy is a cell-death mechanism independent of apoptosis in *Drosophila*; however, this function remains controversial in other organisms and systems.^{49,50} Cell lines have provided extensive information about the function of autophagy by demonstrating that autophagy functions mainly as a cytoprotective mechanism used to preserve cell survival and energy production in adverse conditions.⁵¹ Thus, the autophagy observed in PE placenta may be defensive, in order to turnover damaged organelles in response to oxidative stress milieu experienced by the chorionic villi. This notion is supported by our finding of mitochondrial autophagy, or mitophagy in trophoblast cells and endothelium of PE placentas, suggesting that in this pathological context autophagy is central for recycling damaged mitochondria. In overall, our findings underscore that

Table 1. Clinical features of the study population

	Age-matched controls (n = 18)	Preeclampsia (n = 25)	Term control (n = 10)
Mean maternal Age	32.3 ± 3.8	30.1 ± 5.2	29.8 ± 4.3
Mean gestational age (weeks)	29 ± 3.3 (25 to 35)	28.6 ± 2.86 (24 to 35)	38.6 ± 1.2 (37 to 40)
Blood pressure (mmHg)	Systolic: 112 ± 5.5 Diastolic: 69.1 ± 5.7	Systolic: 174.5 ± 13 Diastolic: 109 ± 12.2	Systolic: 112.7 ± 18.6 Diastolic: 75.5 ± 6.5
Proteinuria (g/24 h)	Absent	3.0 ± 1	Absent
Mean fetal weight (g)	A.G.A. 1488.2 ± 668.2	A.G.A.(80%) 1255 ± 305 IUGR (20%) 802.5 ± 245	A.G.A.3350 ± 275
Mode of delivery	CS 48% VD 52%	CS 88% VD 12%	CS 100%

Data are represented as mean ± standard deviation. A.G.A., appropriate for gestational age; IUGR, intrauterine growth restriction; CS, cesarean section; VD, vaginal delivery.

the BOK-MCL1 system is at the crossroad between life and death pathways in preeclampsia.

Materials and Methods

Cell culture

Human choriocarcinoma JEG3 cells (ATCC, HTB-36) were maintained in EMEM media (ATCC, 30-2003) supplemented with 10% fetal bovine serum (nonheat inactivated) at 20% oxygen (standard conditions). Flp-In T-Rex human embryonic kidney (HEK) cell lines stably expressing either GFP alone (HEK293-GFP) or GFP-hBOK (HEK293-GFP-BOK) were generated as previously described.²³ HEK293-BOK and HEK293-GFP cells were maintained in DMEM high glucose media (Lunenfeld-Tanenbaum Research Institute) with 10% FBS, 0.01% blasticidin (Life Technologies, R210-01), and 0.4% hygromycin (Roche, 10843555001). Expression of BOK-GFP or GFP was induced by doxycycline (2.5 and 5 ng; Sigma-Aldrich, D9891) treatment for different time points (12, 24, and 48 h). Autophagic flux in HEK293-GFP-BOK and control cells was examined by treating the cells with and without 50 nM BafA₁ (Sigma-Aldrich, B1793) for 24 h following BOK induction by doxycycline.

Transfections

Human JEG3 cells were transfected with 3 µg of construct per 35-mm cell culture plate (pcDNA3.1, pcDNA3MCL1, pcDNA3MCL1c127, pcDNA3MCL1c157, pcDNA3MCL1S vectors) using Lipofectamine 2000 (Invitrogen, 11668) as previously described.¹⁶ In parallel experiments, JEG3 cells transiently transfected with MCL1c157 and MCL1c127 constructs were treated with and without 50 nM BafA₁ for 24 h.

SNP treatment

JEG3 cells were seeded into a 6-well cell culture plate (2 × 10⁵ cells per well) and treated for 6 h with 2.5 mM or 5 mM SNP [sodium nitroferricyanide (III); Sigma-Aldrich, 228710]. In a subset of experiments, JEG3 cells in the presence or absence of 2.5 mM SNP were treated with and without 50 nM BafA₁ for 24 h.

MCL1 and BOK siRNA experiments

Silencing of *MCL1* and *BOK* in JEG3 cells was performed with 60 nM of 2 different validated *Silencer Select*[®] siRNA duplexes targeted against mRNA of either *MCL1* (Ambion, 4390824) or *BOK* (Ambion, 4392420) using Lipofectamine 2000. Scrambled siRNA sequences were used as negative control. After transfection, cells were maintained at 20% O₂ for 24 h before protein collection.

Immunofluorescence staining

HEK293-GFP, HEK293-GFP-hBOK, and JEG3 transfected cells were seeded on sterile glass coverslips and allowed to adhere overnight. Cells were then incubated with 50 nM LysoTracker[®] Red (Invitrogen, L-7528) for 1 h, and fixed in 3.7% formaldehyde. Slides were treated with 0.4% DAPI for nuclear detection. Immunofluorescence studies were conducted as previously described²³ using rabbit anti-MCL1 (Santa Cruz Biotechnology, sc-819), mouse anti-SQSTM1/p62 (Santa Cruz Biotechnology, sc-28359), and rabbit anti-cytochrome C (Cell Signaling, 4280) primary antibodies overnight at 4 °C. Fluorophore-conjugated secondary anti-rabbit and anti-mouse antibodies were employed and nuclei were subsequently counterstained with DAPI (4',6-diamidino-2-phenylindole; Invitrogen, D1306). Fluorescence images were viewed and captured using a DeltaVision Deconvolution microscope (Applied Precision).

Human tissue sampling

Preeclamptic, normotensive AMC and term control placental samples were attained after informed consent in accordance with the ethics guidelines of University of Toronto and Mount Sinai Hospital, Toronto, Canada and O.I.R.M-Sant'Anna Hospital, University of Turin, Turin, Italy in accordance with the Helsinki Declaration of 1975. Patients' clinical data are summarized in Table 1. The study groups included singleton pregnancies complicated by severe early-onset PE (E-PE, n = 25). The diagnosis of PE was made according to the following criteria: presence of pregnancy-induced hypertension (systolic ≥ 140 mmHg, diastolic ≥ 90 mmHg) and proteinuria (≥ 300 mg/24 h) after the 20th week of gestation in previously normotensive women.¹⁹ Eighteen AMC and TC placentas were obtained from

normal pregnancies that did not show any signs of PE or other placental disease. Maternal age, gestational age, and parity were comparable between PE and AMC groups. Pregnancies with chromosomal anomalies or notable intrauterine infection were excluded from the study. Patients with diabetes, infections, and kidney disease were also excluded. Samples were collected randomly from central and peripheral placental areas and snap frozen immediately after delivery.

Western blotting

Western blotting was performed as previously described.²³ Rabbit anti-MCL1 (1:500, Santa Cruz Biotechnology, sc-819), rabbit anti-LC3B (1:1000; Abcam, ab48394), rabbit anti-BOK (1:500; Abgent, AP16794), goat anti-ACTB (1:1000; Santa Cruz Biotechnology, sc-1616), mouse anti-SQSTM1/p62 (1:500; Santa Cruz Biotechnology, sc-28359), and anti-mouse GFP (1:1000; B-2, Santa Cruz Biotechnology, sc-9996) were used as primary antibodies and detected using HRP-conjugated secondary antibodies. Detection of HRP-conjugated secondary was performed using ECL plus chemiluminescent reagent (Perkin Elmer, NEL103001EA) and imaged on X-ray film (GE Healthcare) or using the gel-documentation system VersaDoc (Bio-Rad Laboratories).

Immunoprecipitation studies

HEK293-GFP-hBOK and HEK293-GFP stably transfected cells were collected in 1% Triton-x containing a protease inhibitor cocktail. Two-hundred micrograms of cell lysate was rapidly sonicated and incubated at 4 °C overnight with rabbit anti-BECN1 (1:100; Cell Signaling, 3495). Thirty microliters of Protein-A agarose beads (Santa Cruz Biotechnology, sc-2001) were added to the samples and the mixtures were incubated at 4 °C for 3 h. Agarose beads were collected by centrifugation and washed 3 times with PBS. The beads were then resuspended in 2X-SDS loading buffer, boiled for 5 min and centrifuged. The supernatants were collected, subjected to SDS-PAGE and analyzed by western blotting for MCL1 and BECN1. The association between MCL1 and BECN1 in PE placentas and normotensive age-matched controls was examined as previously described.²⁸ Following immunoprecipitation of MCL1 using

anti-MCL1 antibody, immunoprecipitates were subjected to SDS-PAGE and immunoblotted with anti-BECN1 antibody.

Electron microscopy

Placentas from preeclamptic and normotensive control pregnancies were diced into 2-mm pieces within 10 min of delivery and placed into EM fixative (2% glutaraldehyde, 0.1 M sodium cacodylate) for 24 h at 4 °C. Tissues were subsequently processed into thin sections by the Mount Sinai Hospital Electron Microscopy facility. Following doxycycline induction, HEK293-GFP-hBOK, and HEK293-GFP stably transfected cells were treated with EM fixative and stored at 4 °C for 24 h prior to processing for EM by the MSH Electron Microscopy facility. Images were taken using a FEI Tecnai 20 Transmission Electron Microscope (FEI North America NanoPort).

Statistical analysis

All data are presented as mean \pm s.e.m. For comparison of data between multiple groups we used one-way analysis of variance (ANOVA) with posthoc Newman-Keuls multiple comparisons test. For comparison between 2 groups we used paired and unpaired the Student *t* test as appropriate. Statistical tests were performed using Graphpad Prism 5 software and significance was accepted at $P < 0.05$.

Disclosure of Potential Conflicts of Interest

None of the authors has any competing financial interests in relation to the work described in the present manuscript or other conflict of interests.

Acknowledgments

We thank Dr Dragica Curovic for placental collection and the BioBank Program of the CIHR Group in Development and Fetal Health (CIHR #MGC-13299), the Lunenfeld-Tanenbaum Research Institute, and the MSH Department of Obstetrics and Gynaecology for the human specimens used in this study. This work was supported by the Canadian Institutes of Health Research (CIHR) Grant (MOP-89813) to IC. MP is the holder of a Canadian Research Chair (tier 1) in Fetal, Neonatal, and Maternal Health.

References

- Maiuri MC, Le Toumelin G, Criollo A, Rain J-C, Gautier F, Juin P, Tasdemir E, Pierron G, Troulinaki K, Tavernarakis N, et al. Functional and physical interaction between Bcl-X(L) and a BH3-like domain in Beclin-1. *EMBO J* 2007; 26:2527-39; PMID:17446862; <http://dx.doi.org/10.1038/sj.emboj.7601689>
- Scott RC, Schuldiner O, Neufeld TP. Role and regulation of starvation-induced autophagy in the *Drosophila* fat body. *Dev Cell* 2004; 7:167-78; PMID:15296714; <http://dx.doi.org/10.1016/j.devcel.2004.07.009>
- Zhang H, Kong X, Kang J, Su J, Li Y, Zhong J, Sun L. Oxidative stress induces parallel autophagy and mitochondria dysfunction in human glioma U251 cells. *Toxicol Sci* 2009; 110:376-88; PMID:19451193; <http://dx.doi.org/10.1093/toxsci/kfp101>
- Mizushima N, Levine B, Cuervo AM, Klionsky DJ. Autophagy fights disease through cellular self-digestion. *Nature* 2008; 451:1069-75; PMID:18305538; <http://dx.doi.org/10.1038/nature06639>
- Meléndez A, Neufeld TP. The cell biology of autophagy in metazoans: a developing story. *Development* 2008; 135:2347-60; PMID:18567846; <http://dx.doi.org/10.1242/dev.016105>
- Shimizu S, Kanaseki T, Mizushima N, Mizuta T, Arakawa-Kobayashi S, Thompson CB, Tsujimoto Y. Role of Bcl-2 family proteins in a non-apoptotic programmed cell death dependent on autophagy genes. *Nat Cell Biol* 2004; 6:1221-8; PMID:15558033; <http://dx.doi.org/10.1038/ncb1192>
- Chao DT, Korsmeyer SJ. BCL-2 family: regulators of cell death. *Annu Rev Immunol* 1998; 16:395-419; PMID:9597135; <http://dx.doi.org/10.1146/annurev.immunol.16.1.395>
- Heath-Engel HM, Chang NC, Shore GC. The endoplasmic reticulum in apoptosis and autophagy: role of the BCL-2 protein family. *Oncogene* 2008; 27:6419-33; PMID:18955970; <http://dx.doi.org/10.1038/onc.2008.309>
- Oberstein A, Jeffrey PD, Shi Y. Crystal structure of the Bcl-XL-Beclin 1 peptide complex: Beclin 1 is a novel BH3-only protein. *J Biol Chem* 2007; 282:13123-32; PMID:17337444; <http://dx.doi.org/10.1074/jbc.M700492200>
- Liang XH, Jackson S, Seaman M, Brown K, Kempkes B, Hibshoosh H, Levine B. Induction of autophagy and inhibition of tumorigenesis by beclin 1. *Nature* 1999; 402:672-6; PMID:10604474; <http://dx.doi.org/10.1038/45257>
- Erlich S, Mizrachi L, Segev O, Lindenboim L, Zmira O, Adi-Harel S, Hirsch JA, Stein R, Pinkas-Kramarski R. Differential interactions between Beclin 1 and Bcl-2 family members. *Autophagy* 2007; 3:561-8; PMID:17643073
- Germain M, Nguyen AP, Le Grand JN, Arbour N, Vanderluit JL, Park DS, Opferman JT, Slack RS. MCL-1 is a stress sensor that regulates autophagy in a developmentally regulated manner. *EMBO J* 2011; 30:395-407; PMID:21139567; <http://dx.doi.org/10.1038/emboj.2010.327>
- Hsu SY, Kaipia A, McGee E, Lomeli M, Hsueh AJW. Bok is a pro-apoptotic Bcl-2 protein with restricted expression in reproductive tissues and heterodimerizes with selective anti-apoptotic Bcl-2 family members. *Proc Natl Acad Sci U S A* 1997; 94:12401-6; PMID:9356461; <http://dx.doi.org/10.1073/pnas.94.23.12401>

14. Inohara N, Ekhterae D, Garcia I, Carrio R, Merino J, Merry A, Chen S, Núñez G. Mtd, a novel Bcl-2 family member activates apoptosis in the absence of heterodimerization with Bcl-2 and Bcl-XL. *J Biol Chem* 1998; 273:8705-10; PMID:9535847; <http://dx.doi.org/10.1074/jbc.273.15.8705>
15. Hsu SY, Hsueh AJW. A splicing variant of the Bcl-2 member Bok with a truncated BH3 domain induces apoptosis but does not dimerize with antiapoptotic Bcl-2 proteins in vitro. *J Biol Chem* 1998; 273:30139-46; PMID:9804769; <http://dx.doi.org/10.1074/jbc.273.46.30139>
16. Soleymanlou N, Jurisicova A, Wu Y, Chijiwa M, Ray JE, Detmar J, Todros T, Zamudio S, Post M, Caniggia I. Hypoxic switch in mitochondrial myeloid cell leukemia factor-1/Mtd apoptotic rheostat contributes to human trophoblast cell death in preeclampsia. *Am J Pathol* 2007; 171:496-506; PMID:17600131; <http://dx.doi.org/10.2353/ajpath.2007.070094>
17. Bingle CD, Craig RW, Swales BM, Singleton V, Zhou P, Whyte MKB. Exon skipping in Mcl-1 results in a bcl-2 homology domain 3 only gene product that promotes cell death. *J Biol Chem* 2000; 275:22136-46; PMID:10766760; <http://dx.doi.org/10.1074/jbc.M909572199>
18. Day CL, Chen L, Richardson SJ, Harrison PJ, Huang DCS, Hinds MG. Solution structure of pro-survival Mcl-1 and characterization of its binding by proapoptotic BH3-only ligands. *J Biol Chem* 2005; 280:4738-44; PMID:15550399; <http://dx.doi.org/10.1074/jbc.M411434200>
19. ACOG Committee on Practice Bulletins--Obstetrics. ACOG practice bulletin. Diagnosis and management of preeclampsia and eclampsia. Number 33, January 2002. *Obstet Gynecol* 2002; 99:159-67; PMID:16175681
20. Hubel CA. Oxidative stress in the pathogenesis of preeclampsia. *Proc Soc Exp Biol Med* 1999; 222:222-35; PMID:10601881; <http://dx.doi.org/10.1046/j.1525-1373.1999.d01-139.x>
21. Soleymanlou N, Jurisicova I, Nevo O, Ietta F, Zhang X, Zamudio S, Post M, Caniggia I. Molecular evidence of placental hypoxia in preeclampsia. *J Clin Endocrinol Metab* 2005; 90:4299-308; PMID:15840747; <http://dx.doi.org/10.1210/jc.2005-0078>
22. Hung T-H, Burton GJ. Hypoxia and reoxygenation: a possible mechanism for placental oxidative stress in preeclampsia. *Taiwan J Obstet Gynecol* 2006; 45:189-200; PMID:17175463; [http://dx.doi.org/10.1016/S1028-4559\(09\)60224-2](http://dx.doi.org/10.1016/S1028-4559(09)60224-2)
23. Ray JE, Garcia J, Jurisicova A, Caniggia I. Mtd/Bok takes a swing: proapoptotic Mtd/Bok regulates trophoblast cell proliferation during human placental development and in preeclampsia. *Cell Death Differ* 2010; 17: 846-59; PMID:19942931; <http://dx.doi.org/10.1038/cdd.2009.167>
24. Soleymanlou N, Wu Y, Wang JX, Todros T, Ietta F, Jurisicova A, Post M, Caniggia I. A novel Mtd splice isoform is responsible for trophoblast cell death in pre-eclampsia. *Cell Death Differ* 2005; 12:441-52; PMID:15775999; <http://dx.doi.org/10.1038/sj.cdd.4401593>
25. McPhee CK, Logan MA, Freeman MR, Baehrecke EH. Activation of autophagy during cell death requires the engulfment receptor Draper. *Nature* 2010; 465:1093-6; PMID:20577216; <http://dx.doi.org/10.1038/nature09127>
26. Codogno P, Meijer AJ. Autophagy and signaling: their role in cell survival and cell death. *Cell Death Differ* 2005; 12(Suppl 2):1509-18; PMID:16247498; <http://dx.doi.org/10.1038/sj.cdd.4401751>
27. Klionsky DJ, Abeliovich H, Agostinis P, Agrawal DK, Aliev G, Askew DS, Baba M, Baehrecke EH, Bahr BA, Ballabio A, et al. Guidelines for the use and interpretation of assays for monitoring autophagy in higher eukaryotes. *Autophagy* 2008; 4:151-75; PMID:18188003
28. Rolfo A, Garcia J, Todros T, Post M, Caniggia I. The double life of MULE in preeclamptic and IUGR placentae. *Cell Death Dis* 2012; 3:e305; PMID:22552282; <http://dx.doi.org/10.1038/cddis.2012.44>
29. Cardaci S, Filomeni G, Rotilio G, Ciriolo MR. Reactive oxygen species mediate p53 activation and apoptosis induced by sodium nitroprusside in SH-SY5Y cells. *Mol Pharmacol* 2008; 74:1234-45; PMID:18676676; <http://dx.doi.org/10.1124/mol.108.048975>
30. Pattingre S, Tassa A, Qu X, Garuti R, Liang XH, Mizushima N, Packer M, Schneider MD, Levine B. Bcl-2 antiapoptotic proteins inhibit Beclin 1-dependent autophagy. *Cell* 2005; 122:927-39; PMID:16179260; <http://dx.doi.org/10.1016/j.cell.2005.07.002>
31. Levine B, Sinha S, Kroemer G. Bcl-2 family members: dual regulators of apoptosis and autophagy. *Autophagy* 2008; 4:600-6; PMID:18497563
32. Priault M, Hue E, Marhuenda F, Pilet P, Oliver L, Vallette FM. Differential dependence on Beclin 1 for the regulation of pro-survival autophagy by Bcl-2 and Bcl-xL in HCT116 colorectal cancer cells. *PLoS One* 2010; 5:e8755; PMID:20090905; <http://dx.doi.org/10.1371/journal.pone.0008755>
33. Yousefi S, Perozzo R, Schmid I, Ziemiecki A, Schaffner T, Scapozza L, Brunner T, Simon HU. Calpain-mediated cleavage of Atg5 switches autophagy to apoptosis. *Nat Cell Biol* 2006; 8:1124-32; PMID:16998475; <http://dx.doi.org/10.1038/ncb1482>
34. Kang R, Zeh HJ, Lotze MT, Tang D. The Beclin 1 network regulates autophagy and apoptosis. *Cell Death Differ* 2011; 18:571-80; PMID:21311563; <http://dx.doi.org/10.1038/cdd.2010.191>
35. Oh S-Y, Choi S-J, Kim KH, Cho EY, Kim JH, Roh CR. Autophagy-related proteins, LC3 and Beclin-1, in placentas from pregnancies complicated by preeclampsia. *Reprod Sci* 2008; 15:912-20; PMID:19050324; <http://dx.doi.org/10.1177/1933719108319159>
36. Hung TH, Chen SF, Lo LM, Li MJ, Yeh YL, Hsieh TT. Increased autophagy in placentas of intrauterine growth-restricted pregnancies. *PLoS One* 2012; 7:e40957; PMID:22815878; <http://dx.doi.org/10.1371/journal.pone.0040957>
37. Signorelli P, Avagliano L, Virgili E, Gagliostro V, Doi P, Braidotti P, Bulfamante GP, Ghidoni R, Marconi AM. Autophagy in term normal human placentas. *Placenta* 2011; 32:482-5; PMID:21459442; <http://dx.doi.org/10.1016/j.placenta.2011.03.005>
38. Myatt L, Cui X. Oxidative stress in the placenta. *Histochem Cell Biol* 2004; 122:369-82; PMID:15248072; <http://dx.doi.org/10.1007/s00418-004-0677-x>
39. Yang S, Wang X, Contino G, Liesa M, Sahin E, Ying H, Bause A, Li Y, Stommel JM, Dell'antonio G, et al. Pancreatic cancers require autophagy for tumor growth. *Genes Dev* 2011; 25:717-29; PMID:21406549; <http://dx.doi.org/10.1101/gad.2016111>
40. Bonapace L, Bornhauser BC, Schmitz M, Cario G, Ziegler U, Niggli FK, Schäfer BW, Schrappe M, Stanulla M, Bourquin JP. Induction of autophagy-dependent necroptosis is required for childhood acute lymphoblastic leukemia cells to overcome glucocorticoid resistance. *J Clin Invest* 2010; 120:1310-23; PMID:20200450; <http://dx.doi.org/10.1172/JCI39987>
41. Burton GJ, Jones CJP. Syncytial knots, sprouts, apoptosis, and trophoblast deportation from the human placenta. *Taiwan J Obstet Gynecol* 2009; 48:28-37; PMID:19346189; [http://dx.doi.org/10.1016/S1028-4559\(09\)60032-2](http://dx.doi.org/10.1016/S1028-4559(09)60032-2)
42. Huppertz B, Kingdom J, Caniggia I, Desoye G, Black S, Korr H, Kaufmann P. Hypoxia favours necrotic versus apoptotic shedding of placental syncytiotrophoblast into the maternal circulation. *Placenta* 2003; 24:181-90; PMID:12566245; <http://dx.doi.org/10.1053/plac.2002.0903>
43. Sarkar S, Korolchuk VI, Renna M, Imarisio S, Fleming A, Williams A, Garcia-Arencibia M, Rose C, Luo S, Underwood BR, et al. Complex inhibitory effects of nitric oxide on autophagy. *Mol Cell* 2011; 43:19-32; PMID:21726807; <http://dx.doi.org/10.1016/j.molcel.2011.04.029>
44. Lee J, Giordano S, Zhang J. Autophagy, mitochondria and oxidative stress: cross-talk and redox signalling. *Biochem J* 2012; 441:523-40; PMID:22187934; <http://dx.doi.org/10.1042/BJ20111451>
45. Janjetovic K, Misirkic M, Vucicevic L, Harhaji L, Trajkovic V. Synergistic antiangioma action of hyperthermia and nitric oxide. *Eur J Pharmacol* 2008; 583:1-10; PMID:18262519; <http://dx.doi.org/10.1016/j.ejphar.2007.12.028>
46. Barsoum MJ, Yuan H, Gerencser AA, Liot G, Kushnareva Y, Gräber S, Kovacs I, Lee WD, Waggoner J, Cui J, et al. Nitric oxide-induced mitochondrial fission is regulated by dynamin-related GTPases in neurons. *EMBO J* 2006; 25:3900-11; PMID:16874299; <http://dx.doi.org/10.1038/sj.emboj.7601253>
47. Zhang J, Ney PA. Mechanisms and biology of B-cell leukemia/lymphoma 2/adenovirus E1B interacting protein 3 and Nip-like protein X. *Antioxid Redox Signal* 2011; 14:1959-69; PMID:21126215; <http://dx.doi.org/10.1089/ars.2010.3772>
48. Zhang J, Ney PA. Role of BNIP3 and NIX in cell death, autophagy, and mitophagy. *Cell Death Differ* 2009; 16:939-46; PMID:19229244; <http://dx.doi.org/10.1038/cdd.2009.16>
49. Baehrecke EH. Autophagic programmed cell death in Drosophila. *Cell Death Differ* 2003; 10:940-5; PMID:12934068; <http://dx.doi.org/10.1038/sj.cdd.4401280>
50. He C, Levine B. The Beclin 1 interactome. *Curr Opin Cell Biol* 2010; 22:140-9; PMID:20097051; <http://dx.doi.org/10.1016/j.ceb.2010.01.001>
51. Levine B, Yuan J. Autophagy in cell death: an innocent convict? *J Clin Invest* 2005; 115:2679-88; PMID:16200202; <http://dx.doi.org/10.1172/JCI26390>